SOLAR WIND HEAVY IONS FROM FLARE-HEATED CORONAL PLASMA*

S. J. BAME, J. R. ASBRIDGE, W. C. FELDMAN, E. E. FENIMORE, and J. T. GOSLING

University of California, Los Alamos Scientific Laboratory
Los Alamos, N.M. 87545, U.S.A.

(Received 30 May; in revised form 10 November, 1978)

Abstract. Information concerning the coronal expansion is carried by solar wind heavy ions. Distinctly different energy-per-charge ion spectra are found in two classes of solar wind having the low kinetic temperatures necessary for E/q resolution of the ion species. Heavy ion spectra which can be resolved are most frequently observed in the low-speed interstream (IS) plasma found between high speed streams; the streams are thought to be coming from coronal holes. Although the sources of the IS plasma are uncertain, the heavy ion spectra found there contain identifiable peaks of O, Si, and Fe ions. Such spectra indicate that the IS ionization state of O is established in coronal gas at $T \approx 2.1 \times 10^6$ K while that of Fe is frozen in farther out at $\sim 1.5 \times 10^6$ K. On occasion anomalous spectra are found outside IS flows in solar wind with abnormally depressed local kinetic temperatures. The anomalous spectra contain Fe^{16+} ions, not usually found in IS flows, and the derived coronal freezing in temperatures are significantly higher; for two of the best cases values of $\sim 3.4 \times 10^6$ K were found for the O ions and $\sim 2.9 \times 10^6$ K for Fe ions. The coronal sources of some of these ionizationally hot flows are identified as solar flares. The appearance of abnormally depressed kinetic temperatures in solar wind coming from flare-heated coronal gas lends support to earlier speculation that flares can expel plasma enclosed in magnetic bottles or bubbles. In transit to 1 AU the gas is sufficiently isolated from the hot corona that it cools anomalously.

1. Introduction

For ten years, ions heavier than those of helium have been detected in the solar wind using electrostatic analysis (Bame *et al.*, 1968a, 1970; Cattaneo *et al.*, 1971; Grunwaldt, 1976). When the local ion thermal temperatures are low, various ions of O, Si (with some admixture of S), and Fe can be resolved in E/q spectra. Having a common bulk speed, the ion species appear at unique positions determined by ion mass and charge (see e.g. Bame, 1972). When local temperatures are high, as in high speed streams, individual O and Si ion species are not resolved. Whether those of Fe can be resolved is not known. Most frequently, resolved spectra are found in solar wind flows between high speed streams. In this low speed interstream (IS) plasma the ion temperatures are low enough (Strong *et al.*, 1966; Burlaga and Ogilvie, 1970; Hundhausen *et al.*, 1970) that ion species peaks can be identified. We will characterize this class of low speed, low temperature, interstream plasma as 'IS' rather than

Solar Physics **62** (1979) 179–201. 0038–0938/79/0621–0179$03.45.

'quiet' or 'normal' because in some respects the faster solar wind found in high speed streams is more quiet and normal than the slower IS flows (Bame *et al.*, 1977; Feldman *et al.*, 1977).

Because the ionization states of the plasma are established or 'frozen in' at relatively low levels in the corona (Hundhausen *et al.*, 1968a, b; Bame *et al.*, 1974), important information is carried by the heavy ions concerning coronal conditions. Ratios of various heavy ion pairs are frozen in over a range of solar altitudes and coronal temperatures. Under the model conditions of Newkirk (1967), used in Bame *et al.* (1974), the O^{6+}/O^{7+} ion pair ratio freezes in at $T \approx 2.1 \times 10^6$ K near 1.5 solar radii, $R_\odot$. The Si^{9+} to Si^{7+} pair ratios are established in the range ~ 2.4 to $\sim 2.8 R_\odot$, and those of Fe^{13+} to Fe^{7+} in the range ~ 2.6 to $\sim 3.9 R_\odot$ at $\sim 1.5 \times 10^6$ K. These results apply only to the low temperature IS solar wind whose site of origin in the corona is presently uncertain. No information is yet available for the high speed streams, thought to emanate from coronal holes (Krieger *et al.*, 1973, 1974; Nolte *et al.*, 1976; Sheeley *et al.*, 1976; Hundhausen, 1977).

Heavy ion spectra distinctly different from those found in interstream plasma are sometimes observed. Three types of interplanetary conditions have been distinguished when these anomalous spectra are found. They can be categorized as (1) that following a flare-produced interplanetary shock disturbance (Bame *et al.*, 1973, 1978), (2) an enhanced density event not readily attributable to an interplanetary compression (Fenimore *et al.*, 1978), and (3) an enhanced He event with no obvious direct relationship to either (1) or (2) (Fenimore *et al.*, 1978). A more extensive discussion of the second and third classes of interplanetary flows will be presented separately (Fenimore, 1979).

It is the purpose of this paper to concentrate on the flare related events and (1) to present examples of anomalous heavy ion spectra, (2) to show that some of the examples were obtained in flare-related post-shock flows with abnormal temperature depressions as described by Gosling *et al.* (1973) and Montgomery *et al.* (1974), (3) to note and quantify the differences between anomalous and interstream spectra, and (4) to present a self-consistent interpretation of the anomalous spectra showing that the ionization states are frozen in at substantially higher temperatures than normal, presumably within flare-heated and expanding coronal gas.

2. Instrumentation

Hemispherical electrostatic analyzers with special operating modes designed to enhance heavy ion measurements were placed on each of the four Vela-5 and 6 Earth-oriented satellites launched into $20 R_E$ circular orbits in 1969 and 1970. These instruments have higher efficiency than is used for normal solar wind H and He ion measurements, and operate with a multiple sweeping technique which insures that there are no measurement gaps in energy or angle except for small gaps between the four sweep ranges used to give four sets of 20 contiguous counting samples over an E/q range of 1 to 8 kV. This range, chosen to maximize the yield of useful spectra

from the slow IS solar wind, is sometimes insufficient to cover the entire E/q range of the anomalous spectra.

Only a limited amount of useful heavy ion data has been accumulated due to a number of factors. The spacecraft must be actively tracked; commonly this is one hour out of four. At $20R_E$ the spacecraft are in the solar wind only $\sim\frac{1}{3}$ time and much of this time the Earth-oriented spin axis direction is inappropriate. Substantial parts of the data have to be rejected because of contamination by upstream protons from the bow shock (Asbridge *et al.*, 1968) and because of inappropriate solar wind conditions. The heavy ion analyzers operate part of the time in a non-heavy-ion mode. Thus, even though the instruments have accumulated data over years of operating time, a frustratingly modest yield of useful data has been produced, especially for the infrequent anamolous events considered here. Further details of the instrumentation can be found in Bame (1972).

3. Observations

3.1. Anomalous 'hot' spectra of 1971, May 18 and 1970, November 19

The heavy ion data from the early years of operation of the Vela-5 and 6 plasma analyzers have been used in studies concerning the composition at 1 AU and the temperature and temperature gradient of those parts of the corona expanding to form the IS solar wind (Bame *et al.*, 1974, 1975). Generally, when the temperature is low and the speed and its fluctuations are low, resolvable heavy ion spectra like the upper spectrum in Figure 1 are found. This measurement was made in solar wind with a speed of 365 km s^{-1}, a proton density of ~ 6 cm^{-3}, and a proton temperature of $\sim 25 \times 10^3$ K. It is an observational fact that the measured ion species E/q positions are those expected if all species share a nearly equal bulk speed. Thus, the E/q scale can be converted directly to an M/q scale which here is labelled with the ion species positions for ease of inspection. This spectrum is typical of IS spectra which are characterized by a third most prominent ion peak, O^{6+}, marked *B*. The three peaks marked *C*, *D*, and *E* are predominantly Si^{9+}, Si^{8+}, and Si^{7+} ions and are followed by Fe ion peaks ranging from Fe^{13+} to Fe^{7+}. All peaks beyond He have similar narrow widths, usually close to the instrumental resolution width. At times when the peaks are broader but still resolved, they all appear to have about the same width within experimental accuracy. Thus, peak heights can be used to judge the relative intensities of the various species. If the He peak is narrow, a peak of O^{7+} ions at position *A* is resolved. Other examples of IS spectra can be found in Bame *et al.* (1970, 1974, 1975), Bame (1972), and Feldman *et al.* (1974).

A number of anomalous spectra have been found having distinctly different characteristics than IS spectra. An example, measured on 1971, May 18, is shown in Figure 1. As will be shown, the ionization state of this example, obtained in a post-shock temperature-depressed solar wind flow following a solar flare, was formed at temperatures higher than usual, so it is labelled 'hot'.

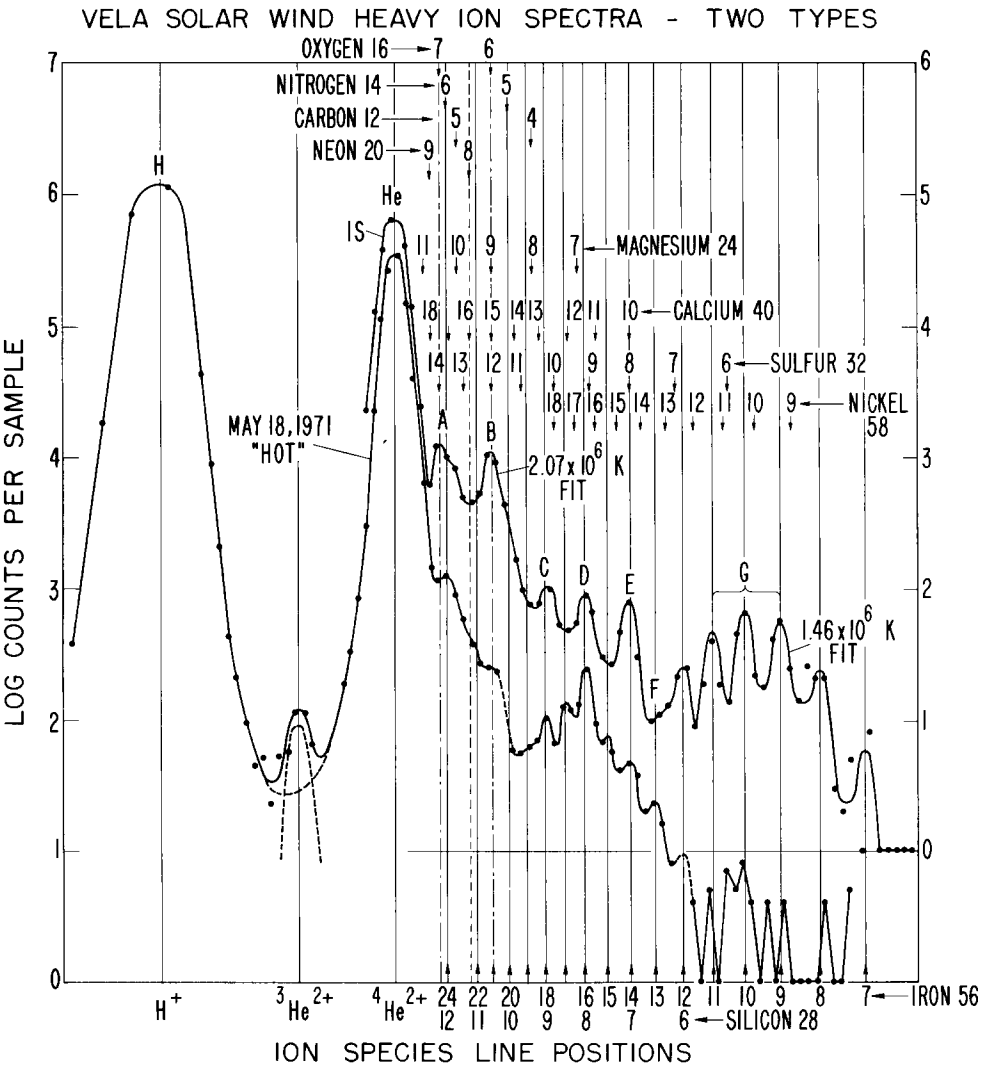

Fig. 1. A heavy ion spectrum from the interstream low speed, low temperature (IS) solar wind of 1969, June 23 (upper spectrum) measured with Vela-5A between 03:26 UT and 04:22 UT and an anomalous 'hot' spectrum measured with Vela-6B on 1971, May 18, between 02:38 UT and 04:29 UT. In the region of the He and O^{7+} peaks of the IS spectrum, data from 1970, September 27, have been used as an aid in providing better resolution of the O^{7+} peak in this sample spectrum.

Distinct differences between the hot and IS spectra are apparent. Some cases of intermediate spectra have also been observed (see also Fenimore, 1979). The normally prominent O^{6+} peak at *B*, is very subdued in the hot spectrum; on the other hand, a prominent peak occurs at *D* which will be shown to be principally Fe^{16+} ions. In IS spectra the O^{7+} and O^{6+} ion peaks at *A* and *B* are of comparable intensity; in the hot spectrum there is no completely resolved peak at *B* and the peak level at *A* is

very high compared to the level at *B*. In some hot spectra O^{6+} is better resolved than here, but the *A*/*B* intensity ratio is still high relative to IS spectrum ratios.

In the IS spectrum the three silicon (sulfur) lines at *C*, *D*, and *E* have similar intensities and are well defined with no discernable peaks between them; in contrast, the hot spectrum has more peaks in this range with highly different intensities. Another distinguishing feature of the hot spectrum is the radical depression of the level of the Fe peaks in the range marked *G* in the figure. Some hot spectra do not exhibit as great a depression as here, but the group is generally low compared to levels in the *C*, *D*, *E* range. A *G*-level depression cannot be determined for some hot spectra when the bulk speed is so high that the *G* peaks lie above 8 kV/q.

The example in Figure 1 is one of a few in which the H and He ion peak widths and counting statistics permit resolution of the solar wind $^3He^{2+}$ ions (see also Bame *et al.*, 1968a). Here the $^3He^{2+}$ to $^4He^{2+}$ number ratio is $\sim 3 \times 10^{-4}$ as compared to an average value of 4.3×10^{-4} determined with the Apollo foil measurements (Geiss *et al.*, 1972).

Several additional anomalous spectra from an event on 1970, November 19 are shown in Figure 2. The top spectrum is very similar to the hot spectrum of Figure 1, having a prominent presumed Fe^{16+} peak, a depressed O^{6+} peak, and a *G* range depression. The other two spectra show a time evolution from the earlier one. They have similar features but the Fe^{16+} ion peaks are not as pronounced and more O^{6+} seems to be present. As was the case for the 1971, May 18 spectrum, the November 19 spectra were also measured in a post-shock flow as discussed below.

3.2. Flare related post-shock flow events of may 1971 and november 1970

The following sequence of events, partly extracted from the NOAA *Solar-Geophysical Data* reports shows that the spectrum of 1971, May 18 was obtained in flare-expelled plasma driving an interplanetary shock. On May 14, starting at ~14:10 UT, a flare or series of flares variously reported as importance 1B to 3B was observed at 04° N and 11° E (McMath region 11312). No comparable flares were observed during the following two days. The flare was accompanied by an X-ray emission event at ~ 14:12 UT and by type II and IV radio bursts, often associated with flare produced shock waves (see Hundhausen, 1972). Skylab results show that these bursts are almost invariably accompanied by mass ejections (Gosling *et al.*, 1974). A small solar energetic particle event was observed with the Vela neutron monitors on May 14 with an onset at ~14:40 UT. A larger energetic particle event and a type IV radio burst on May 16 occurred too late to be associated with an interplanetary shock observed with the LASL plasma experiment on IMP-6 at ~06:30 UT on May 17. A highly probable association for this shock is with the ~14:30 UT flare event of May 14, yielding a shock transit time of 64 hr. Earthbound measurements also indicated the passage of an interplanetary shock. An SC was observed at 06:29 UT on May 17, initiating a major geomagnetic storm, and a Forbush decrease was observed.

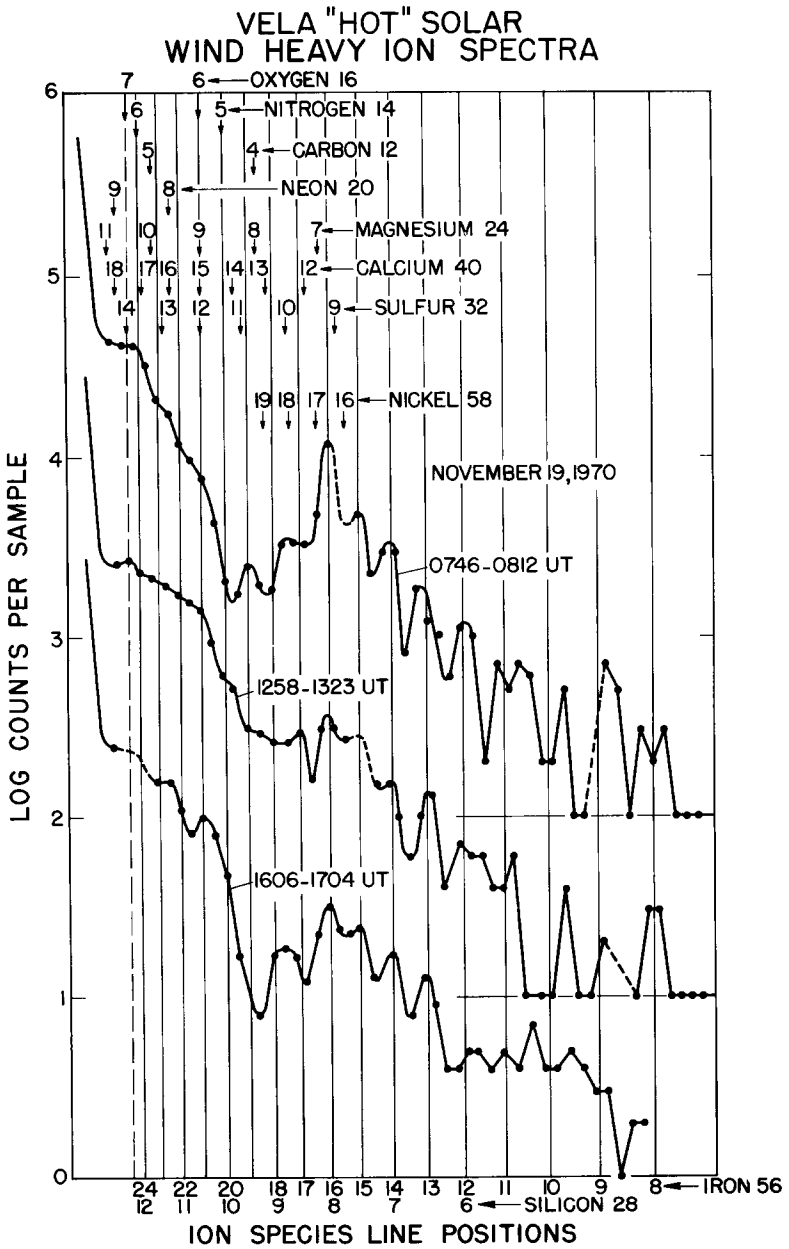

Fig. 2. Hot heavy ion spectra obtained on 1970, November 19. The spectra are displaced from each other by factors of 10. Data points from spectrum to spectrum do not necessarily line up because of shifts in speed.

An interplanetary record of the event is given in Figure 3. About 10 hr after the shock on May 17 (74 hr from flare maximum) several major changes occurred in the solar wind flow. Such changes have been associated with the arrival of gas from

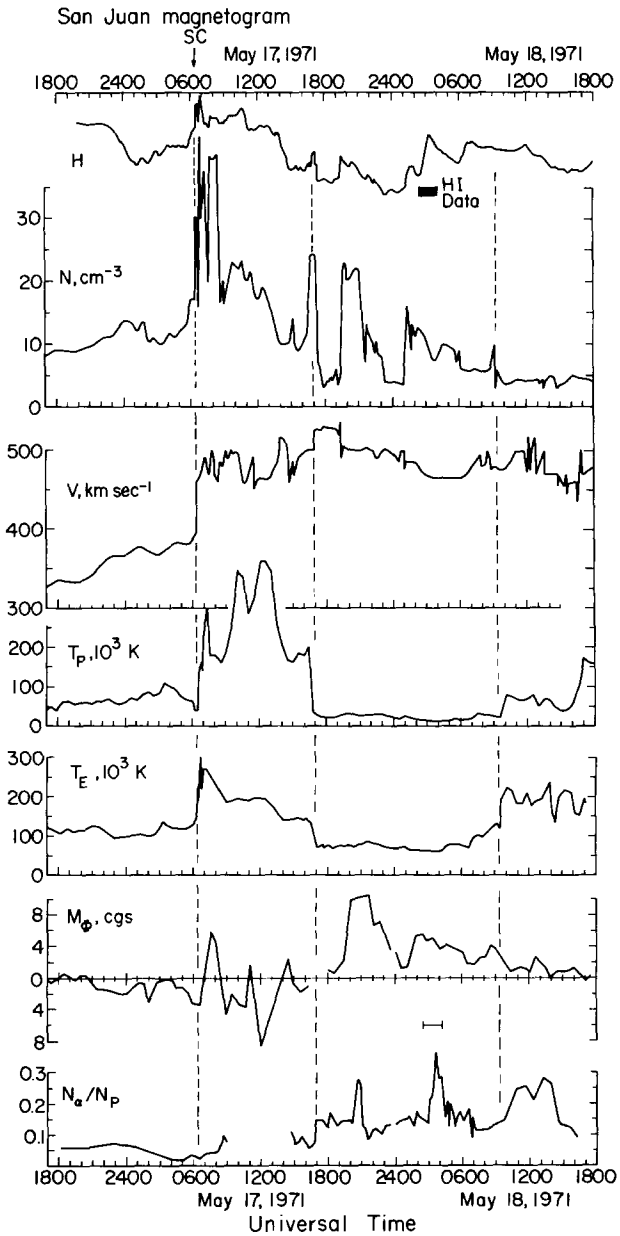

Fig. 3. History of interplanetary solar wind changes during the 1971, May sequence of events measured with the LASL plasma spectrometer on IMP-6. N, V, and T_p are the solar wind proton density, bulk speed, and temperature. T_E is the solar wind electron temperature, M is the angular momentum flux, and N_α/N_p is the number ratio of He and H ions.

the flare region on the basis of interpretations of Vela and IMP data. A large depression in the proton temperature T_p occurred with an abrupt onset at ~17:00 UT, coincident with a depression in the electron temperature, a density peak, a sudden

increase in speed, and a marked feature in the geomagnetogram. Abnormal depressions of T_p like this to values well below those usually measured at this bulk speed have been observed in association with the interplanetary shocks numerous times with Vela plasma analyzers (Gosling *et al.*, 1973). Following shocks by ~6–18 hr, they have been inferred to mark the passages of new bodies of solar plasma past the Earth – i.e. the piston gas or flare ejecta driving the shock. It is postulated that the anomalously low T_p is evidence for a magnetic bottle geometry, which isolates the plasma and allows it to cool more than usual in transit to 1 AU. A similar explanation has been offered for T_E depressions which sometimes follow the passage of flare associated interplanetary shocks (Montgomery *et al.*, 1974). Another feature frequently associated with the arrival of flare gas is seen here: A well-defined density spike occurs coincident with the leading edge of the temperature depression (Bame *et al.*, 1978).

Another important feature of the post-shock plasma flow of May 17–18 is the helium enhancement with onset coincident with the leading edge of the temperature depression. Enhancements of N_α/N_p to 12% or more following shocks have been recognized for a decade as marking the arrival of flare driver gas (e.g. Hirschberg *et al.*, 1970, 1972). A possible explanation for the enrichment is that the flare piston gas originates in lower levels of the solar atmosphere than does the normal solar wind (Hirschberg *et al.*, 1972) where He may be enriched. (A discussion of these possibilities including references to the theoretical work can be found in Hirshberg *et al.* (1972) and in Hirshberg (1973).) Interestingly, this He enhancement extends beyond the temperature depression, suggesting that the inferred magnetic bubble does not necessarily encompass all of the plasma heated and driven out by the flare.

It should be noted that not all post-shock flows exhibit temperature depressions and He enhancements (e.g. Ogilvie and Burlaga, 1974). Presumably in some cases the shock can pass a point in space which is subsequently not engulfed by the driver plasma due either to the particular shock-driver-observer geometry or to deflections of the shock and driver gas in interplanetary space (e.g. Heinemann and Siscoe, 1974; Hirshberg *et al.*, 1974). Possibly the magnetic bottle or bubble is not created in some cases.

Taking into account the May 17 observation of a shock, followed ~10 hr later by temperature depressions and a He enhancement, there is little doubt that the plasma observed beyond ~17:00 UT was a body of plasma heated and expelled from the corona by a solar flare – probably the flare at ~14:30 UT on May 14. The Vela heavy ion measurement was made during the temperature depression and coincides with a peak in the He abundance (see Figure 3). Firm reasons then exist for supposing that this sample of gas should have a hotter ionization state than usual.

Most of the features observed in association with the May 1971 event were also seen in the November 1970 event. A 2B flare was observed on November 16 accompanied by type II and IV radio bursts and by a small solar energetic particle event. About 59 hr after the flare an SC was observed followed by a geomagnetic storm and Forbush decrease. Unfortunately, we must rely on the less extensive

measurements of Vela, shown in Figure 4, for the interplanetary plasma characteristics of this event since IMP-6 was not yet in orbit. An interplanetary shock passed the Earth at ~12:30 UT on November 18. About 10 hr later there was an abrupt decrease in the proton density and what may have been the beginning of a depression of T_p and T_E. Unfortunately, data gaps make it impossible to give a complete history of the interplanetary plasma changes, but there are enough data to show that broad depressions of both T_p and T_E occurred, possibly lasting for 24 hr or

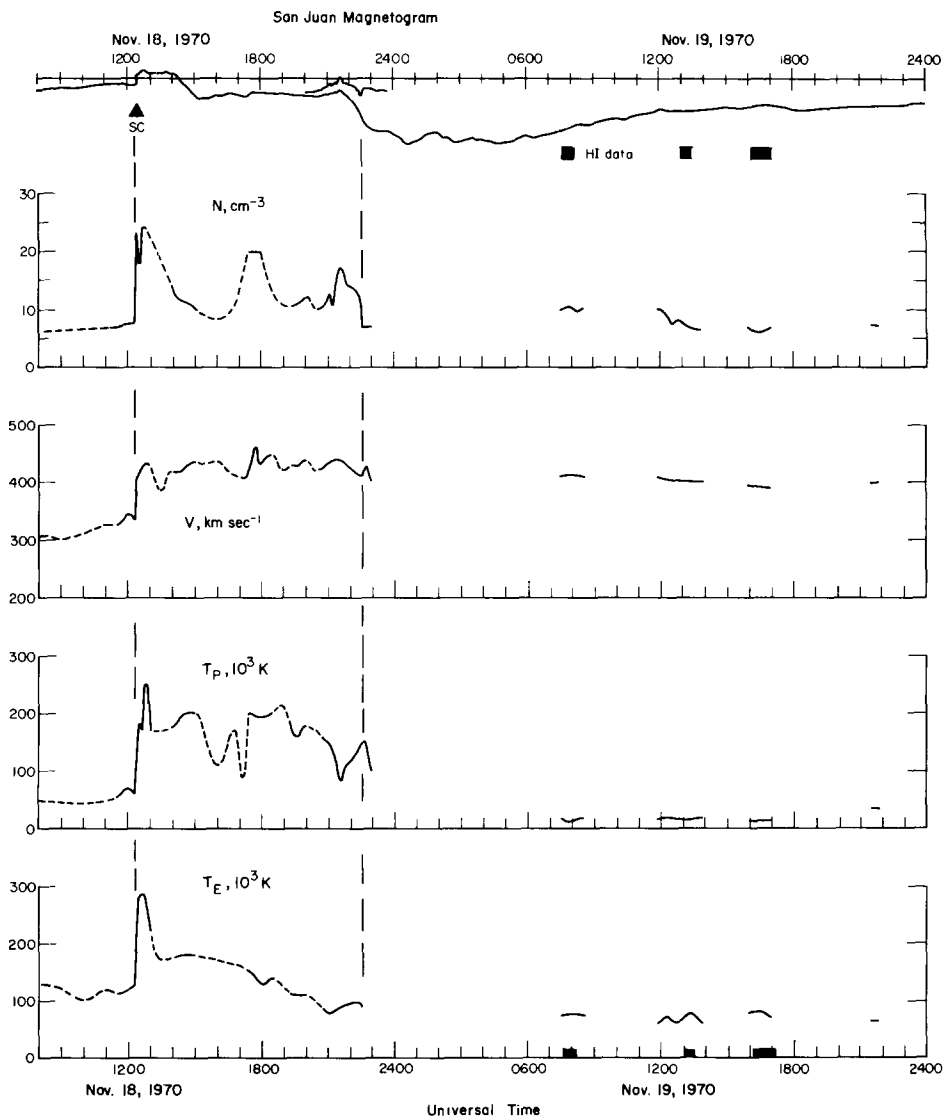

Fig. 4. Sequence of events during which the heavy ion data of 1970, November 19, were obtained. The times of heavy ion measurement are shown by the bars near the top and on the bottom scale.

longer. The heavy ion measurements shown in Figure 2 were obtained in the temperature depression. The He abundance, not shown here, had values fluctuating between 9% and 18%.

Taking these observations into account, it seems almost certain that the heavy ion measurements of 1970, November 19, were made in post-shock temperature-depressed plasma, heated and expelled by a flare on November 16.

3.3. Other observations

In several ways the November 1970 and May 1971 events are the most complete examples of anomalous heavy ion spectra in association with flare events which we have found in the data thus far. Solar wind speed fluctuations were moderate enough that multiple data samples could be combined, taking into account speed changes. Although the measurements were made following IP shocks, the speeds were still low enough that the E/q measurement range encompassed all of the significant ion species. Unfortunately, due to factors discussed in the instrumentation section, only a very limited number of useful spectrum measurements have been obtained in the relatively rare post-shock flows. Additional Vela-5 and 6 examples of hot spectra with flare associations, measured on 1973, April 14, and 1974, September 19, have prominent peaks in the presumed Fe^{16+} position, but due to high solar wind speeds significant portions of the spectra fall above the E/q range of measurement.

Surveying some of the older Vela-3 events, measured with wider energy spacings and less efficiency than those of Vela-5 and 6, probable cases can be made that hot spectra were present during some post-shock flows previously studied. For example, spectra measured during the helium-enhanced, flare-associated, post-shock flow of 1967, January 14, (Bame *et al.*, 1968b) show evidence that the counts in the Fe^{16+} position were anomalously high relative to the O^{6+} position, indicating a hot spectrum. Similar cases can be made for several events during the series of flare-related post-shock flows occurring in late May 1967 (Ogilvie *et al.*, 1968; Hirshberg *et al.*, 1972). On 1966, September 1, following a large flare on August 28, a spectrum was observed with a very high O^{7+}/O^{6+} number ratio and with higher counts at the Fe^{16+} position than at the O^{6+} position, again indicating a hot spectrum.

Even though the number of examples is not large we can be reasonably certain that hot heavy ion spectra are a frequent feature of flare-related, post-shock solar wind flows. However, the detailed morphology of such events must remain uncertain at present due to the paucity of heavy ion measurements. It is known that great variations occur in the appearance of temperature depressions and He enhancements in post-shock flows (e.g. Bame *et al.*, 1978). Of particular interest is the case of a T_p depression following an IP shock on 1972, March 6. A Vela heavy ion measurement made within the depression early on March 8 showed a spectrum with characteristics more like those of a normal IS spectrum than a hot one. Also, at the time, the He abundance was not enhanced. Thus, caution should be used in assuming that an unmeasured post-shock feature is present because another feature has been identified. Records of many more events are needed.

4. Analysis and Discussion

4.1. Quantification of Heavy Ion Spectrum Characteristics

In order to demonstrate that normal IS spectra and hot spectra have distinctly different states, various ion pair intensity ratios, selected to emphasize the differences, have been calculated and are shown in Figure 5. The ion species which can occupy the specific lettered peak positions can be identified by reference to Figure 1.

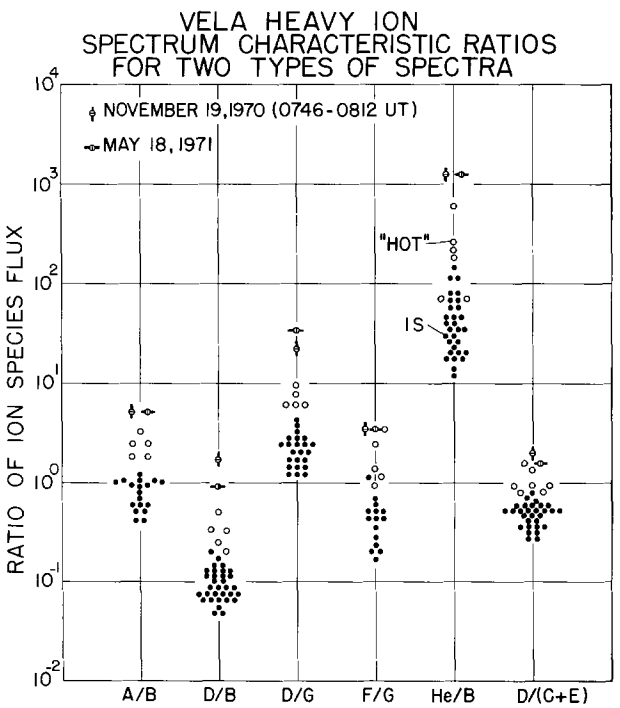

Fig. 5. Vela heavy ion spectrum characteristic ratios for IS and hot spectra. Ratio values have been shifted slightly for ease of plotting. See Figure 1 for identifications of the letter ratios. G is the average of the Fe^{11+}, Fe^{10+}, and Fe^{9+} peak heights.

Ratios were calculated for 30 IS spectra, including all of the examples used in previously reported studies. The spectra are from 19 different days spread over a period of years. Not all ratios can be calculated for some spectra. For example, A/B cannot be estimated for 11 of the spectra because the He peaks obscure the O^{7+} peaks. Ratios were also calculated for five flare-associated hot spectra including the four in Figures 1 and 2 and one measured on 1973, April 14. In addition, the ratios for two temperature-depressed hot spectra measured in May 1970 and April 1971 for which we have not found flare associations are included. Finally, two values of $D/(C+E)$ were obtained from flare-associated hot spectra measured on 1974, September 19.

It is readily seen that the IS and selected hot spectra represent distinctly different states of solar wind plasma. Intermediate spectra are also found but they are more likely to be associated with flows other than flare-related, post-shock flows (Feldman, 1979). Especially high contrast is noted for the hot spectrum of 1971, May 18, and the earliest spectrum of 1970, November 19 (see Figure 5).

4.2. Synthesized heavy ion spectra

Because of the association of some of the anomalous spectra with flare-expelled plasma, it seems likely that their ionization states are frozen in at higher than normal coronal temperatures. To test and quantify this hypothesis, we have synthesized heavy ion spectra over a range of temperatures for comparison with the data. Ultimately it will be desirable to fit the spectra to models of the expanding gas from flares; insight could well be obtained concerning details of the expansion. However, for the present, considering the uncertainties of solar flare expansion models and the lack of agreement between various ionization state calculations, we have chosen to compare the experimental spectra with spectra synthesized under the assumption of a common freezing in temperature for all the ion species. It is important to keep in mind that the various ion ratios actually freeze in over a range of temperatures.

To generate the spectra we adopted the coronal abundances of Withbroe (1976) supplemented with solar wind measured abundances of Si and Fe relative to O (Bame *et al.*, 1975), as shown in Table I. Density independent ionization state calculations of Jordan (1969, 1970) were used and supplemented with those of Mewe (1972) where necessary, because they formed a more complete set than others available to us. From the abundances and the ionization states, peak intensities of the various ion species were calculated as functions of temperature; those for the more abundant ions are shown in Figure 6. Then the synthesized spectra were formed for various freezing in temperatures by giving all peaks the appropriate abundances and ionization state amplitudes, locating them in the spectra according to their M/q positions under the assumption of a common bulk speed, and finally summing all the peaks together. The resulting spectra are presented in Figure 7.

Letters mark the appropriate peaks in the 1.58×10^6 K spectrum for comparison with the IS spectrum in Figure 1. There is a remarkable similarity between the

TABLE I

Relative solar wind abundance values used for synthesizing heavy ion spectra

Element	Abundance	Element	Abundance	Element	Abundance
C	135	Al	0.7	Ti	0.4
N	28	Si	14	Cr	0.9
O	100	S	3.8	Mn	0.4
Ne	9	Ar	0.4	Fe	10
Na	7	K	0.1	Ni	0.7
Mg	10	Ca	0.8		

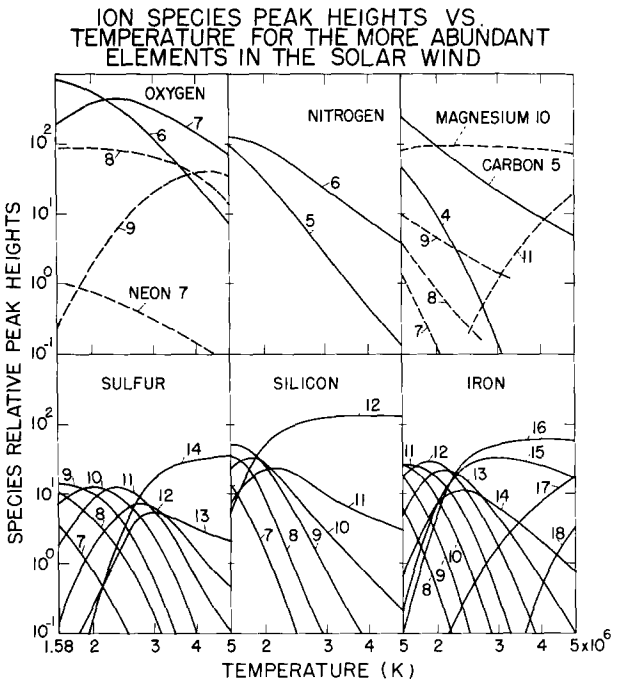

Fig. 6. Ion species peak heights vs freezing in temperature for the more abundant solar wind ions. Ionization states of Jordan were used with the Table I adopted abundances.

synthesized and observed spectra except in the area of the A and B (O^{7+}/O^{6+}) peaks. This exception is understandable because in an expanding, non-isothermal corona the O^{7+}/O^{6+} ratio for IS solar wind freezes in at $\sim 2.1 \times 10^6$ K on the average while the Fe peaks freeze in near 1.5×10^6 K (Bame *et al.*, 1974). Thus, the O peaks are more properly compared to the 2.00×10^6 K spectrum. For the IS spectrum in Figure 1, good fits to the data were obtained using Figures 6 and 7 with $T = 2.07 \times 10^6$ K for the O peaks and with $T = 1.46 \times 10^6$ K for the Fe peaks. Thus, if proper account is taken of the fact that different ion pairs freeze in at different altitudes and temperatures in the corona, the synthesized spectra can be used as an aid in interpreting the experimental spectra. In this regard it should be noted that the C^{4+} and C^{5+} peaks in the 1.26 and 1.58×10^6 K spectra have been arbitrarily reduced to give better comparisons with IS spectra because the C state is established at even higher temperatures than the O state. For T above 2×10^6 most of the C is fully ionized and under the He peak.

Inspection of Figures 6 and 7 illuminates some of the differences between IS and hot spectra. As T increases, the Fe species shift into more highly ionized positions; Fe^{16+} becomes a very prominent peak over a broad temperature range extending from under 3 to above 5×10^6 K. Although the peak height at D contains only $\sim 0.2\%$ Fe^{16+} at 1.58×10^6 K, by 2.51×10^6 K the peak is more than 90% Fe^{16+}. Similarly, as T increases beyond 1.58×10^6 K, ions of Si, S, Mg, Ca, etc., shift into

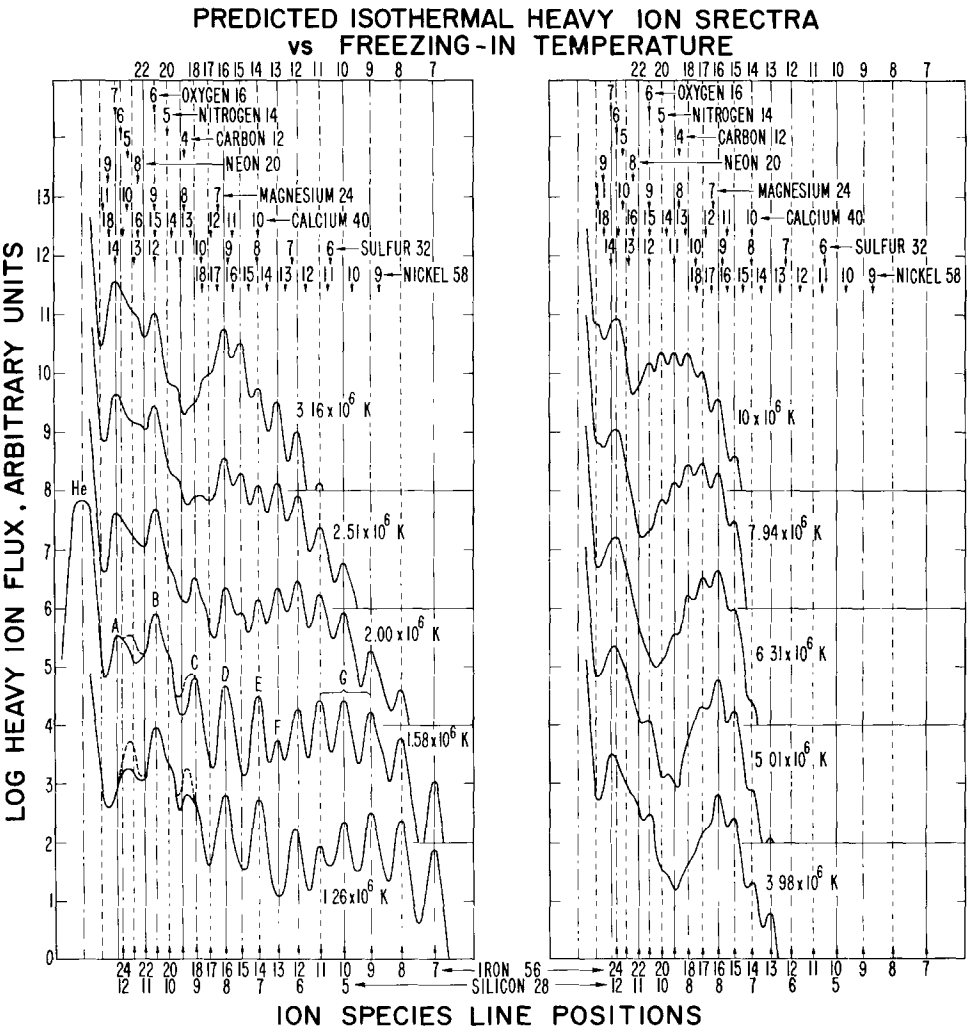

Fig. 7. Heavy ion spectra synthesized using the solar wind abundances in Table I, the Jordan density independent ionization states, and single freezing in temperatures for all species. Spectra are plotted on an M/q scale marked with ion species positions. The freezing in temperature is shown for each spectrum, and the spectra are shown displaced from each other by two decades for clarity.

more highly ionized stages, and out of the *C*, *D*, and *E* positions. At temperatures above 2.5×10^6 K major fractions of the Si and S ions are Si^{12+} and S^{14+} located near the O^{7+} position. Beyond $\sim 1.8 \times 10^6$ K the Fe^{15+} species begins to be resolvable, accounting for one of the additional peaks found in hot spectra.

Comparisons in the range 2.51 to 3.16×10^6 K show remarkable similarities between measured hot spectra and synthesized spectra. The experimental spectra seem to have more ions in the lower ionization stages of Fe; this is probably due in part to the fact that the actual state is formed in an expanding plasma with a

temperature gradient, rather than in an isothermal plasma. Also in some cases there may be mixing of hotter and cooler spectra. It seems reasonable to conclude on the basis of self-consistency that the hot spectra indeed contain Fe^{16+} and Fe^{15+} and of course even higher Fe ions if the ionization temperature is high enough.

Ratios of the lettered position peak heights for the synthesized spectra are shown in Figure 8 and can be compared with the experimental ratios in Figure 5. Although too strict a comparison is probably unwarranted, inspection of the two figures along with Figures 1, 2, 6, and 7 further demonstrates that the ionization states of the anomalous spectra are indeed formed at higher coronal temperatures. A few specific details of the comparisons are worthy of mention here.

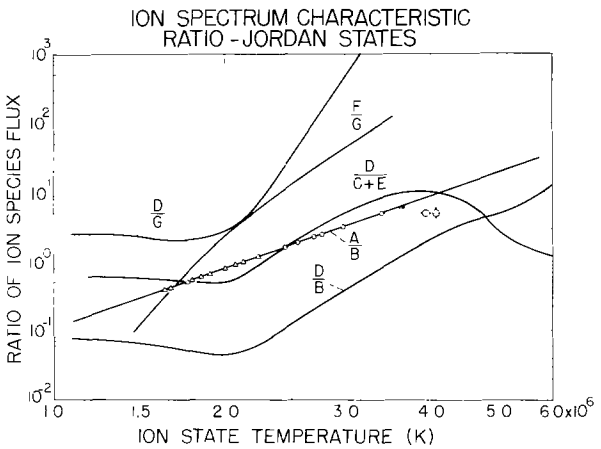

Fig. 8. Letter ratios derived from the synthesized spectra. Experimental A/B ratio points are shown plotted – triangles for IS spectra and circles for hot. Where points overlap only one is plotted, as for the Figure 1 and 2 'hot' examples, marked by the symbols.

As T increases ions of O convert to the higher +7 and +8 stages while Si ions convert to the +12 stage. This results in a steady increase of the A/B ratio, shown in Figure 8. As O^{7+} passes its peak intensity Si^{12+} continues to grow, resulting in a shift in the A-peak position toward Si^{12+} at $T > 3 \times 10^6$ K. This effect is apparent in the synthesized spectra of Figure 7 and can also be noted in the hotter experimental spectra of Figures 1 and 2.

Other features which can be used to identify hot spectra are the D/B and D/G ratios, for reasons understandable by inspection of the various figures. Finally, at higher T where Fe^{16+} is prominent, the $D/(C+E)$ ratio provides a useful indicator of hot spectra for those cases when high speed causes part of the spectrum to be lost above the top of the measurement range.

4.3. Freezing in Temperatures of the Interstream Solar Wind

By comparing measured spectra with synthesized spectra, coronal freezing in temperatures for various ions can be estimated. Results of such an analysis for IS

plasma are presented in Table II. O^{7+}/O^{6+} temperatures were determined using the A/B curve in Figure 8, a technique that takes into account contaminant ions such as Si^{12+} in the O^{7+} peak to first order. The Fe ion temperature estimates were made by comparing the experimental peak intensities with synthesized intensities over a range of species, Fe^{12+} to Fe^{8+}. Less accuracy results if a single ion pair is used. Estimates made with the ionization states of Jordan (1969, 1970), JO, Allen and Dupree (1969), AD, and Jacobs *et al.* (1977), JA, gave values which agree with one another reasonably well. It is not surprising that the JA states gave somewhat lower values because they were calculated using a proposed mechanism by which dielectronic recombination is greatly inhibited.

TABLE II

Freezing in temperatures for low speed, low temperature interstream solar wind heavy ion spectra, derived from comparisons with the synthesized spectra

		Freezing in temperature			
	O^{7+}/O^{6+} temperature	Fe^{12+}–Fe^{8+} peaks (10^6 K)			
Date	(10^6 K)	JO	AD	JA	1974
6–22–69	1.9	–	–	–	–
6–23–69	2.1	1.46	1.48	1.35	1.47
7–06–69	2.1	1.41	1.43	1.30	1.56
1–11–70	2.2	–	–	–	–
2–08–70	1.8	1.50	1.53	1.38	–
5–27–70	2.1	1.58	1.58	1.43	1.64
9–27–70	2.1	1.41	1.43	1.30	1.40
9–27–70	2.0	1.32	1.36	1.23	–
11–22–70	2.1	1.48	1.51	1.38	–
2–21–71	–	1.41	1.43	1.30	–
4–19–71	2.1	–	–	–	–
9–11–71	–	1.23	1.29	1.15	1.29
12–29–71	2.1	–	–	–	–
3–05–72	2.1	–	–	–	–
1–08–75	1.7	–	–	–	–
Average	2.0	1.42	1.45	1.31	1.47

Included in the last column of Table II are Fe temperature values calculated using an expanding model of the corona (Bame *et al.*, 1974). The agreement with other values in the table is reasonably good. Expanding model calculations of O^{7+}/O^{6+} temperatures also agree well with the values given in the table. Thus, since there is no universally accepted expansion model for flare-expelled plasma, it seems reasonable to compare the experimental hot spectra with the synthesized spectra to estimate the temperatures.

4.4. Freezing in temperatures of anomalous hot spectra

The O^{7+}/O^{6+} temperatures for hot spectra were also obtained using the A/B curve of Figure 8. Results are shown in Table III. Determinations of temperatures for the Fe ions were not as straightforward. It was quickly evident that for the hot spectra estimates, using single ion pairs gave widely divergent values depending both on the ion pair chosen and on the ionization state used. It was necessary to make the peak intensity comparisons over a range of peaks – in this case the Fe^{16+} to Fe^{13+} peaks. Even so, agreement between the three estimates using the different ionization calculations is much worse at these higher temperatures than for IS spectra.

TABLE III

Freezing in temperatures for Vela hot heavy ion spectra, derived by comparison with synthesized spectra

Date	O^{7+}/O^{6+} temperature (10^6 K)	Fe^{16+}–Fe^{13+} temperature (10^6 K)		
	JO	JO	AD	JA
5–18–71	3.4	3.0	3.4	2.6
11–19–70(1)	3.4	2.8	3.2	2.4
11–19–70(2)	2.6	2.5	2.7	2.1
11–19–70(3)	2.8	2.5	2.7	2.1
4–14–73	2.5	2.7	3.0	2.3
5–18–70	3.0	2.8	3.2	2.5
4–28–71	2.7	2.8	3.1	2.4
Average	2.9	2.7	3.0	2.3

To illustrate the problem of estimating the Fe temperatures, we have combined the four hot spectra of Figures 1 and 2 in pairs to give two spectra, 'Vela' and '11–19–70', with better statistics for comparison with the JO, AD, and JA ionization states. Normalizing to the Fe^{16+} peak, the peak intensities of the Vela spectrum, which is a combination of the 5–18–71 and 11–19–70 (1) spectra, are 1.00 ± 0.05, 0.35 ± 0.03, 0.24 ± 0.03, 0.13 ± 0.02, and 0.07 ± 0.01 for the peaks of Fe^{16+} to Fe^{12+} in descending order. For the 11–19–70 spectrum, which is a combination of the 11–19–70 (2) and (3) spectra, the intensities in the same order are 1.0 ± 0.12, 0.8 ± 0.11, 0.5 ± 0.09, 0.4 ± 0.08, and 0.2 ± 0.05.

Comparisons of these spectra have been made with spectra synthesized using each of the three available sets of ionization states. Results are shown in Figure 9, in which the 'Vela' experimental spectrum is plotted three times, close to synthesized spectra judged to provide nearly the best possible fits. For the 11–19–70 spectrum only the peak intensity points are shown, plotted superimposed on three synthesized spectra judged to provide nearly best possible fits. For each set, a third higher temperature

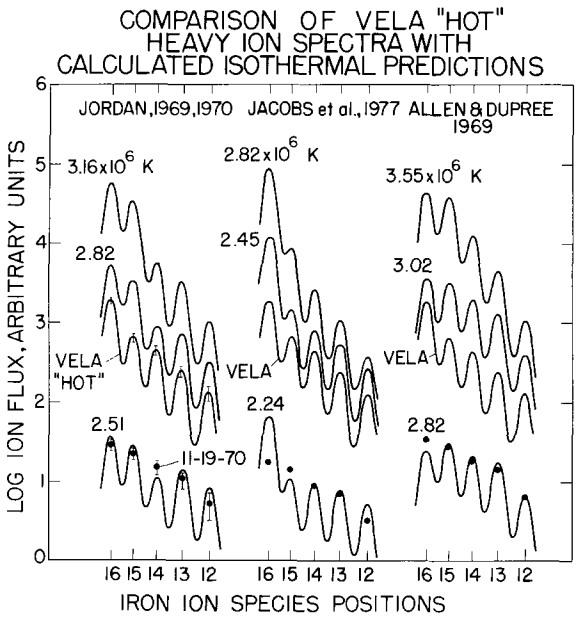

Fig. 9. Comparison of the Vela and 11–19–70 combined spectra with synthesized spectra. The spectra are arbitrarily displaced from each other for clarity.

synthesized spectrum is given to show how the spectral shapes evolve. Best fit temperatures are slightly different from those in the figure. For the Vela spectrum they are 2.9, 2.5, and 3.3×10^6 K for the JO, JA, and AD states respectively. For the 11–19–70 spectrum they are 2.5, 2.1, and 2.7×10^6 K.

Inspection of Figure 9 reveals significant differences in the way the three sets of states compare with the data. None of them appears to be capable of giving a really close fit. We judge that the JO states come closest and this is one of the reasons for using them to synthesize the spectra shown in Figure 7. Perhaps the most obvious discrepancy is with the JA states in which Fe^{16+} seems to be much too prominent. It seems unlikely that a realistic expansion model of flare gas can be found in which integration of any of the presently available ionization equations could produce spectra which compare precisely with the experimental spectra.

4.5. Abundances in flare-expelled plasma

It is of interest to try to determine if there are any major differences in the compositions of flare-expelled plasma and IS plasma. For normal IS solar wind E/q spectra it is usually possible to estimate the abundances of He, O, Si, and Fe by taking into account the measured distribution of identified peaks, estimating contaminants using the coronal abundances, and calculating the unresolved fractions of each element. Abundances from 17 IS spectra determined by Bame *et al.* (1975) are summarized in Table IV and compared with abundances from the hot spectra shown

TABLE IV

Solar wind abundance ratios in flare-expelled plasma compared with average values for interstream plasma

Date	Abundance number ratios				
	He/H $\times 10^{-2}$	O/H $\times 10^{-4}$	Si/H $\times 10^{-5}$	Fe/H $\times 10^{-5}$	Fe/He $\times 10^{-3}$
11–19–70(1)	14	10	–	11.3	0.8
11–19–70(2)	9	6.2	–	12.1	1.3
11–19–70(3)	12	4.3	–	7.2	0.6
5–18–71	12	3.5	–	5.8	0.6
Average	12	6.0	–	9.1	0.8
Interstream					
Maximum	5.3	8.4	11.7	13.9	6.9
Minimum	1.3	1.9	2.8	1.4	0.5
Average	3.3	5.2	7.5	5.3	1.9

in Figures 1 and 2. Fairly accurate estimates for He and Fe could be made because their peaks are very little contaminated. Less accurate values were obtained for O which is contaminated by a number of ion species. No values could be obtained for Si, of course.

The data sample is very limited, so only tentative differences can be discerned between the abundances of IS and flare plasma, except for the firmly established He enrichment of flare gas. There may be an enrichment in Fe also, but smaller percentagewise than that of He. Final determinations must await more extensive measurements.

5. Summary and Conclusions

Two distinct varieties of heavy ion spectra have been found in two kinds of low temperature solar wind (1) the low speed, low temperature interstream (IS) solar wind found between high speed streams, and (2) the temperature-depressed solar wind of any speed. (This is not intended to exclude the possibility of other varieties, classes or subclasses being found.) In the IS plasma the spectra exhibit resolved ion species of O, Si, and Fe in ionization states from which coronal freezing in temperatures of formation can be estimated. Table II summarizes IS temperature determinations. For Fe ionization temperatures, only small differences are found between values calculated using the ionization equilibrium calculations of Jordan (1969, 1970), JO, Allen and Dupree (1969), AD, and Jacobs *et al.* (1977), JA.

In the temperature-depressed solar wind, anomalous heavy ion spectra have been found containing ions which are interpreted to be Fe^{16+} ions; Fe^{16+} is not detected in the IS wind. Ions of O^{6+} are greatly depressed in number as are Fe ions in the range Fe^{11+}–Fe^{7+}. The ionization state freezing in temperatures of these 'hot' spectra,

shown in Table III, are significantly higher than for the IS solar wind. Some of the hot spectra are found in flare-related post-shock solar wind flows. Others have been interpreted to result from non-flare energetic coronal events (Fenimore *et al.*, 1978; Fenimore, 1979). In addition, hot spectra have been observed which suggest that the states were formed over a very broad range of temperatures or that states with different temperatures have become mixed. Agreement between values determined with the three sets of ionization states is not as good in this higher temperature range as at lower temperatures. Each of the sets has deficiencies that may prevent precise fitting even in an appropriate expansion model. When more accurate calculations of recombination and ionization coefficients become available there could be significant changes in the absolute values of the derived temperatures, but not in the conclusion that the ionization state of flare-expelled plasma is frozen in at higher than usual coronal temperatures.

Based on the flare-related hot spectra and IMP observations of a number of post-shock flows (Bame *et al.*, 1978), the following phenomenological picture of flare heated and expelled coronal gas emerges as illustrated in Figure 10. Coronal gas is heated by a flare and explosively expelled, driving an interplanetary shock. Often a high density shell of gas is at the leading edge of the ejecta, as can be inferred for the May 1971 example shown in Figure 3. (High density loops driven out by flares and other energetic coronal events were observed with the Skylab coronagraph (Gosling *et al.*, 1974). The heated plasma is enriched in helium, not uniformly, but with a 'lumpy' distribution. Observation at 1 AU of an ionizationally hot plasma, ~10 hr after the shock passage, identifies the gas driving the shock as that ejected by the flare. Concurrent observation of abnormal depressions of the proton and electron local temperature in a gas which originated in the corona at a higher than usual temperature lends credence to the postulated (Gosling *et al.*, 1973; Montgomery *et al.*, 1974) magnetic bottle and/or bubble geometry of flare-expelled solar wind gas. Plasma enclosed in an isolated bubble or in a bottle with inhibited heat conduction from the corona can be expected to cool anomalously as it expands and flows to 1 AU. Some of the abnormal cooling might also result from a greater than r^{-2} divergence of the flare gas. Different levels of temperature depression are frequently observed in post-shock flare gas flows, suggesting that both bubbles and bottles with inhibited connection may exist. In the Figure 3 case, for example, after T_p has increased to an intermediate level from its lowest depression, high levels of N_α/N_p persist. A possible explanation of this is shown in Figure 10 by the helium enriched plug extending from closed field line regions into regions connecting back into the corona.

With second and third generation heavy ion observations using improved instruments, spectra will be resolved in at least one additional class of solar wind – the high speed streams thought to emanate from coronal holes. In streams, thermal temperatures are too high for individual ion species of O and Si to be E/q resolved. It is not known whether those of Fe^{7+} to Fe^{12+} might be resolvable because the Vela E/q range does not cover those ions when the speed is high. Extrapolating from results

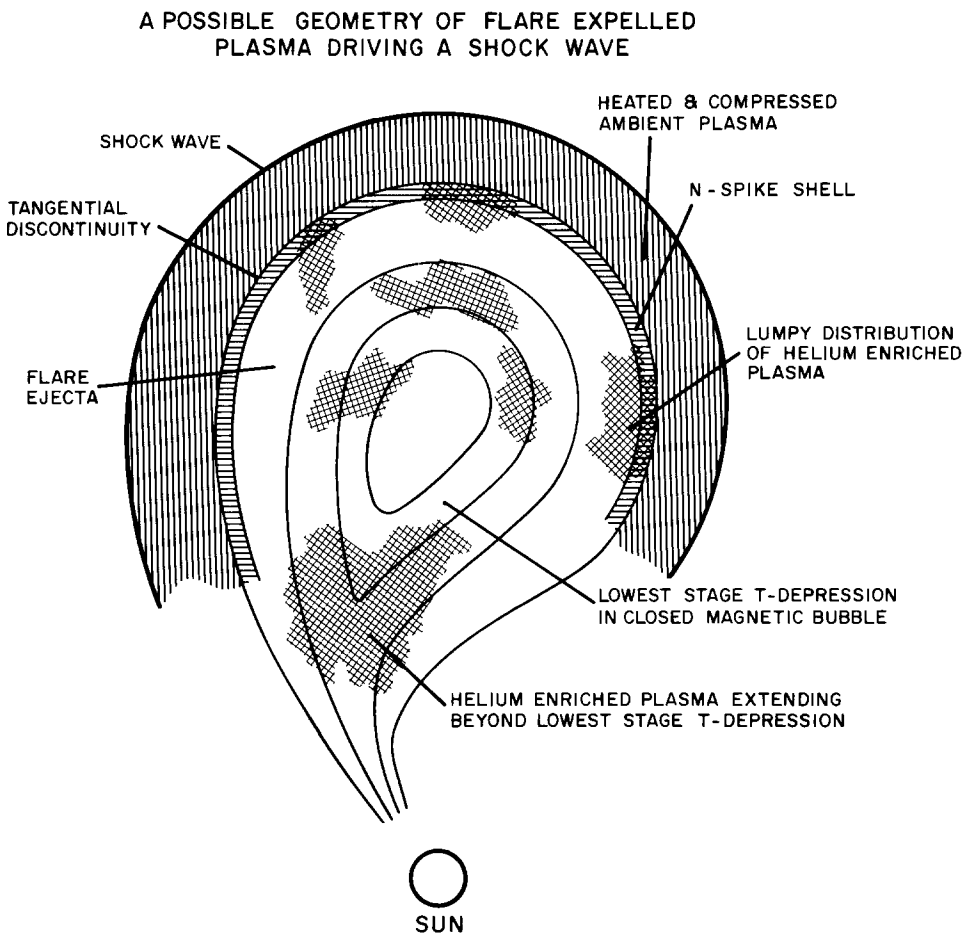

Fig. 10. A possible geometry of flare-expelled plasma driving an interplanetary shock wave. In this extension of the model of Hundhausen (1972), based on the present results and those of Bame *et al.* (1978), the interplanetary field lines threading the shock and compressed ambient plasma have been omitted for clarity; possible magnetic bubble and bottle configurations in the flare-expelled gas are shown.

showing the helium abundance to be much more stable in high speed streams than in the interstream plasma (Bame *et al.*, 1977), it seems likely that the abundances of the heavier ions will be less variable in streams.

Acknowledgements

Significant portions of this research were performed as part of the Vela satellite program, jointly sponsored by the U.S. Department of Defense and the U.S. Department of Energy. The program is managed by the U.S. Air Force and satellite operation activities are under the jurisdiction of the Air Force Satellite Control

Facility. Portions of the data are from the NASA IMP satellite program. This work was done under the auspices of the Department of Energy with support in part by NASA.

References

Allen, J. W. and Dupree, A. K.: 1969, *Astrophys. J.* **155**, 27.
Asbridge, J. R., Bame, S. J., and Strong, I. B.: 1968, *J. Geophys. Res.* **73**, 5777.
Bame, S. J.: 1972, in C. P. Sonett *et al.* (eds.), *Solar Wind*, NASA SP-308, p. 535.
Bame, S. J., Hundhausen, A. J., Asbridge, J. R., and Strong, I. B.: 1968a, *Phys. Rev. Letters* **20**, 393.
Bame, S. J., Asbridge, J. R., Hundhausen, A. J., and Strong, I. B.: 1968b, *J. Geophys. Res.* **73**, 5761.
Bame, S. J., Asbridge, J. R., Hundhausen, A. J., and Montgomery, M. D.: 1970, *J. Geophys. Res.* **75**, 6360.
Bame, S. J., Asbridge, J. R., Feldman, W. C., and Kearney, P. D.: 1973, *Am. Geophys. Union, EOS* **54**, 438.
Bame, S. J., Asbridge, J. R., Feldman, W. C., and Kearney, P. D.: 1974, *Solar Phys.* **35**, 137.
Bame, S. J., Asbridge, J. R., Feldman, W. C., Montgomery, M. D., and Kearney, P. D.: 1975, *Solar Phys.* **43**, 463.
Bame, S. J., Asbridge, J. R., Feldman, W. C., and Gosling, J. T.: 1977, *J. Geophys. Res.* **82**, 1487.
Bame, S. J., Asbridge, J. R., Feldman, W. C., Fenimore, E., and Gosling, J. T.: 1978, *Trans. Am. Geophys. Union, EOS* **59**, 368.
Burlaga, L. F. and Ogilvie, K. W.: 1970, *Astrophys. J.* **159**, 659.
Cattaneo, M. B., Formisano, V., Moreno, G., Palmiotto, F., Palutan, F., Saraceno, P.: 1971, *Solar Phys.* **17**, 468.
Feldman, W. C., Asbridge, J. R., Bame, S. J., and Kearney, P. D.: 1974, *J. Geophys. Res.* **79**, 1808.
Feldman, W. C., Asbridge, J. R., Bame, S. J., and Gosling, J. T.: 1977 in O. R. White (ed.), *The Solar Output and its Variation*, Colorado Associated Press, Boulder, p. 351.
Fenimore, E.: 1979, in preparation.
Fenimore, E., Asbridge, J. R., Bame, S. J., Feldman, W. C., and Gosling, J. T.: 1978, *Trans. Am. Geophys. Union, EOS* **59**, 368.
Geiss, J., Buhler, F., Cerutti, H., and Eberhardt, P.: 1972, NASA SP-289, 15-1.
Gosling, J. T., Pizzo, V., and Bame, S. J.: 1973, *J. Geophys. Res.* **78**, 2001.
Gosling, J. T., Hildner, E., MacQueen, R. M., Munro, R. H., Poland, A. I., and Ross, C. L.: 1974, *J. Geophys. Res.* **79**, 4581.
Grunwaldt, H.: 1976, *Space Research* **XVI**, 681.
Heinemann, M. A. and Siscoe, G. L.: 1974, *J. Geophys. Res.* **79**, 1349.
Hirshberg, J.: 1973, *Rev. Geophys. Space Phys.* **11**, 115.
Hirshberg, J., Alksne, A., Colburn, D. S., Bame, S. J., and Hundhausen, A. J.: 1970, *J. Geophys. Res.* **75**, 1.
Hirshberg, J., Bame, S. J., and Robbins, D. E.: 1972, *Solar Phys.* **23**, 467.
Hirshberg, J., Nakagawa, Y., and Wellck, R. E.: 1974, *J. Geophys. Res.* **79**, 3726.
Hundhausen, A. J.: 1972, in C. P. Sonett *et al.* (eds.), *Solar Wind*, NASA SP-308, p. 393.
Hundhausen, A. J.: 1977, J. B. Zirker (ed.), in *Coronal Holes and High Speed Wind Streams*, Colorado Associated University Press, p. 225.
Hundhausen, A. J., Gilbert, H. E., and Bame, S. J.: 1968a, *Astrophys. J.* **152**, L3.
Hundhausen, A. J., Gilbert, H. E., and Bame, S. J.: 1968b, *J. Geophys. Res.* **73**, 5485.
Hundhausen, A. J., Bame, S. J., Asbridge, J. R., and Sydoriak, S. J.: 1970, *J. Geophys. Res.* **75**, 4643.
Jacobs, V. L., Davis, J., Kepple, P. C., and Blaha, M.: 1977, *Astrophys. J.* **211**, 605.
Jordan, C.: 1969, *Monthly Notices Roy. Astron. Soc.* **142**, 501.
Jordan, C.: 1970, *Monthly Notices Roy. Astron. Soc.* **148**, 17.
Krieger, A. S., Timothy, A. F., and Roelof, E. C.: 1973, *Solar Phys.* **29**, 505.
Krieger, A. S., Timothy, A. F., Vaiana, G. S., Lazarus, A. J., and Sullivan, J. D.: 1974, in C. T. Russell (ed.), *Solar Wind Three*, p. 132, University of California Press, Los Angeles.
Mewe, R.: 1972, *Solar Phys.* **22**, 459.
Montgomery, M. D., Asbridge, J. R., Bame, S. J., and Feldman, W. C.: 1974, *J. Geophys. Res.* **79**, 3103.

Newkirk, G., Jr.: 1967, *Ann. Rev. Astron. Astrophys.* **5**, 213.
Nolte, J. T., Krieger, A. S., Timothy, A. F., Gold, R. E., Roelof, E. C., Vaiana, G., Lazarus, A. J., Sullivan, J. D., and McIntosh, P. S.: 1976, *Solar Phys.* **46**, 303.
Ogilvie, K. W., Burlaga, L. F., and Wilkerson, T. D.: 1968, *J. Geophys. Res.* **73**, 6809.
Ogilvie, K. W. and Burlaga, L. F.: 1974, *J. Geophys. Res.* **79**, 2324.
Sheeley, N. R., Jr., Harvey, J. W., and Feldman, W. C.: 1976, *Solar Phys.* **49**, 271.
Strong, I. B., Asbridge, J. R., Bame, S. J., Heckman, H. H., and Hundhausen, A. J.: 1966, *Phys. Rev. Letters* **16**, 631.
Withbroe, G. L.: 1976, Harvard College Observatory Preprint Series No. 524.